Liquid Mixtures of Xenon with Fluorinated Species: Xenon + Sulfur Hexafluoride

Lino M. B. Dias,[†,§] Eduardo J. M. Filipe,[*,†] Clare McCabe,[‡] Telma Cordeiro,[†] and Jorge C. G. Calado[*,†]

Centro de Química Estrutural, Instituto Superior Técnico, 1049-001 Lisboa, Portugal, Department of Chemical Engineering, Vanderbilt University, Nashville, Tennessee 37235

Received: August 12, 2006; In Final Form: November 29, 2006

The vapor−liquid equilibrium of binary mixtures of xenon + SF_6 has been measured at nine temperatures from 235.34 to 295.79 K and pressures up to 6.5 MPa. The mixture critical line is found to be continuous between the critical points of the pure components, and hence, the system can be classified as type I phase behavior in the scheme of van Konynenburg and Scott. The excess Gibbs free energies have been calculated, and the experimental results have been interpreted using the statistical associating fluid theory for potentials of variable range (SAFT-VR). Additionally, the SAFT-VR equation has been used to model other systems involving SF_6 and alkanes, illustrating the predictability of the approach and further demonstrating the transferability of parameters between binary mixtures involving alkanes and xenon.

1. Introduction

Over the past two decades, considerable research effort has focused on understanding the influence of molecular structure, shape, polarity, and flexibility on the thermodynamic properties and phase behavior of binary liquid mixtures. The strategy has been to investigate systems that are as close as possible to theoretical models, meticulously selecting the pairs of molecules under study, so that the contribution of each factor can be individually assessed. For example, when probing electrostatic effects, molecular shape should be kept as simple as possible (preferably spherical), and ideally, each component should have only one multipole moment of considerable magnitude. Using this methodology, many of the possible combinations of multipole moments in binary mixtures have been studied, such as nonpolar + dipolar through the xenon + CH_3F system,[1] nonpolar + quadrupolar with xenon + N_2O[2], and nonpolar + octopolar with xenon + CF_4[3], etc.

The present work deals with the thermodynamics of binary mixtures of xenon and sulfur hexafluoride (SF_6). Xenon is a spherical nonpolar particle with a high polarizability that enhances dispersion forces and displays a liquid range that overlaps comfortably with that of sulfur hexafluoride. SF_6 is a fully fluorinated octahedral molecule whose first nonzero multipole moment is the hexadecapole ($\mu = 1.8 \times 10^{-59}$ C m^4). Since the influence of hexadecapoles on excess properties is expected to be almost negligible, this system thus represents an excellent case with which to assess nonpolar + perfluoro contributions in the absence of multipole moments. Moreover, sulfur hexafluoride is a nontoxic and nonflammable substance, making it a possible solvent, either as a pure fluid or mixed with carbon dioxide, for supercritical extraction technology.

From a theoretical point of view, a major step in our understanding of liquid mixtures has been the development of molecularly based equations of state, such as the perturbed hard chain theory[4] and the statistical associating fluid theory (SAFT).[5,6] Unlike typical engineering or cubic equations of state, these tools explicitly take into account the contribution of molecular details, such as nonsphericity (molecular shape), polarity, and association interactions, providing a powerful and successful method to study the effects of molecular interactions on the thermodynamics and phase behavior of fluids. In recent work, we have reported results on the thermodynamic properties of liquid mixtures of xenon with the lower alkanes[7−9] and perfluoroalkanes.[10,11] Using a combined experimental and theoretical approach through the SAFT-VR equation (a version of the SAFT approach that treats associating and nonassociating chain molecules that interact through dispersion potentials of variable attractive range), we have highlighted the similarities that exist between xenon and the alkanes. In particular, we found that the SAFT-VR parameters obtained for xenon by fitting to experimental vapor pressure and saturated liquid density data lie within the average value of those used to describe the *n*-alkanes, implying that xenon can be represented as a sphere with almost the same diameter and potential as those suited to describe the *n*-alkanes.[6] Our work has also shown that, in general, the behavior of mixtures of an *n*-alkane with a second component is mirrored by that of xenon with that same component[12] and that the unlike interaction parameters (i.e., deviations from the Lorentz−Berthelot combining rules) can be used interchangeably between mixtures involving xenon and those involving *n*-alkanes, eliminating the need to fit to experimental mixture data and providing a fully predictive approach. We further explore this behavior in the current work.

Here we report vapor−liquid equilibrium measurements for binary mixtures of xenon + SF_6 at nine temperatures from 235.34 to 295.79 K and at pressures up to 6.5 MPa; the isotherm at the lowest temperature is only 13 K above the triple point temperature of SF_6 (222.4 K); therefore, this study covers most of the binary mixture liquid range. The mixture critical line has been located and is shown to be continuous, with a temperature minimum between the critical points of the pure components. The phase equilibria results were interpreted using the SAFT-VR equation. The vapor−liquid equilibrium diagram, including

* Corresponding author. E-mail: efilipe@ist.utl.pt; jcalado@ist.utl.pt.
† Instituto Superior Técnico.
‡ Vanderbilt University.
§ Present address: Bayer CropScience AG, PMSCM-BS Process Improvement, 40789 Monheim am Rhein, Germany.

10.1021/jp065222j CCC: $37.00
Published on Web 04/21/2007

TABLE 1: Experimental *p, T, x, y, R_p,* and G^E Vapor−Liquid Equilibrium Results for xXe + $(1 - x)$$SF_6$ Binary Mixtures at Temperatures below the Critical Temperature of Xenon[a]

p (MPa)	x (Xe)	y (Xe)	$y - y_{calcd}$	R_p (Pa)	G^E(J mol^{-1})
		235.34 K			
0.368	0	0			0
0.513	0.0525	0.2769	0.0113	−0.271	76.3
0.719	0.1303	0.4882	0.0115	0.313	187.4
0.903	0.2231	0.6066	0.0086	−0.175	282.9
1.021	0.2867	0.6660	0.0022	0.035	341.6
1.249	0.4485	0.7548	−0.0018	−0.028	428.2
1.399	0.5907	0.8128	−0.0083	0.053	436.7
1.515	0.7354	0.8580	−0.0051	−0.040	366.0
1.587	0.8442	0.8971	−0.0002	−0.019	256.7
1.613	0.8862	0.9176	0.0005	0.062	201.4
1.620	0.9038	0.9279	0.0001	0.017	173.8
1.624	0.9105	0.9342	−0.0021	0.022	163.4
1.639	0.9564	0.9630	−0.0001	−0.092	82.9
1.650	1	1			0
		250.32 K			
0.625	0	0			0
0.965	0.0837	0.3438	0.0032	0.305	135.9
1.382	0.2391	0.5654	−0.0072	−0.408	296.1
1.705	0.3902	0.6714	−0.0080	0.023	382.0
1.997	0.5552	0.7627	−0.0158	0.453	397.5
2.198	0.7038	0.8274	−0.0124	0.126	334.8
2.288	0.7866	0.8610	−0.0056	−0.138	269.3
2.336	0.8352	0.8841	−0.0025	−0.197	221.7
2.378	0.8870	0.9137	−0.0013	−0.289	161.3
2.416	0.9328	0.9423	0.0014	−0.024	104.5
2.442	1	1			0
		265.35 K			
0.993	0	0			0
1.399	0.1035	0.2882	0.0120	−0.229	95.3
1.818	0.2078	0.4629	0.0080	0.120	188.5
2.208	0.3175	0.5743	0.0030	0.274	265.1
2.604	0.4591	0.6701	−0.0044	−0.193	315.2
2.908	0.5923	0.7434	−0.0112	−0.256	313.6
3.228	0.7638	0.8325	−0.0101	0.011	236.5
3.313	0.8197	0.8656	−0.0083	0.151	193.9
3.416	0.9117	0.9222	0.0017	0.209	104.8
3.466	1	1	-	-	0

[a] y_{calcd} is the mole fraction of xenon in the gas phase, R_p is the pressure residuals ($p - p_{calcd}$), and G^E is the excess molar Gibbs energy, calculated using Barker's method.

TABLE 2: Experimental *p, T, x, y* vapor−liquid Equilibrium Results for x Xe + $(1 - x)$ SF_6 Binary Mixtures at Temperatures between the Critical Temperature of Xenon and Sulfur Hexafluoride

p (MPa)	x(Xe)	y (Xe)	p (MPa)	x (Xe)	y (Xe)
	280.85 K			291.31 K	
1.535	0	0	2.007	0	0
2.003	0.0915	0.2269	2.438	0.0761	0.1689
2.542	0.2086	0.3956	3.026	0.1819	0.3241
3.009	0.3230	0.4969	3.589	0.3012	0.4289
3.212	0.3754	0.5381	4.035	0.3920	0.4989
3.785	0.5266	0.6467	4.555	0.5029	0.5631
4.203	0.6563	0.7311	4.623	0.5197	0.5701
4.674	0.8524	0.8673	4.719	0.5415	0.5799
3.486	0.4444	0.5873	4.734	0.5477	0.5795
4.347	0.7057	0.7616	*4.90*	*0.59*	*0.59*
4.611	0.8152	0.8386			
4.778	0.9091	0.9169			
4.822	1	1			
	287.29 K			295.75 K	
4.701	0.6417	0.6848	2.208	0	0
4.902	0.6982	0.7213	2.617	0.0724	0.1409
4.936	0.7086	0.7269	2.987	0.1392	0.2442
5.01	*0.73*	*0.73*	3.228	0.1837	0.2988
5.48	*0.93*	*0.93*	3.780	0.2836	0.3911
5.491	0.9371	0.9398	4.047	0.3349	0.4320
5.517	0.9792	0.9842	4.421	0.4084	0.4793
5.520	0.9885	0.9916	4.642	0.4625	0.4968
5.523	0.9994	0.9996	*4.79*	*0.50*	*0.50*
5.525	1	1			
	289.26 K			305.27 K	
4.208	0.4672	0.5595	2.791	0	0
4.553	0.5467	0.6079	3.045	0.0423	0.0712
4.820	0.6083	0.6379	3.200	0.0656	0.1068
4.96	*0.64*	*0.64*	3.424	0.1037	0.1575
			3.581	0.1310	0.1891
			3.754	0.1611	0.2208
			4.057	0.2148	0.2665
			4.267	0.2531	0.2892
			4.167	0.2374	0.2811
			4.365	0.2700	0.2959
			4.386	0.2750	0.2973
			4.52	*0.30*	*0.30*

[a] x is the xenon mole fraction in the liquid phase; y is the xenon mole fraction in the vapor phase. For each isotherm, the critical point is shown in italics.

the critical region, has been predicted. The theoretical study also confirms the type I classification[13] for the xenon + SF_6 phase diagram and is used to draw further comparisons between xenon and alkane systems. As far as we are aware, no prior thermodynamic study has been performed on this system.

2. Experimental Section

The apparatus and experimental method have recently been described in detail.[9] The equilibrium cell, based on the equipment used by Streett and Calado,[14] consists essentially of a transparent thick-walled glass cell of approximately 14 cm^3 capacity, immersed in a commercial cryogenic bath. The glass cell has the advantage of allowing a visual detection of the vapor−liquid critical point of the mixture, making use of the characteristic opalescence observed near the critical point, but sets an upper limit to the accessible pressure range of ∼8 MPa. In the cell, close contact between the vapor and liquid phases is guaranteed by the strong stirring of the liquid, which is achieved using a Teflon-coated magnet actuated by an immersed magnetic stirrer. The total volume of the lines connecting the equilibrium cell to the pressure transducer, made of 0.03-in.-i.d. stainless steel tubings, is very small as compared to the total volume of the vapor phase. Capillary lines are used to withdraw small samples of liquid and vapor after equilibrium is reached in the cell. The samples are then passed through a thermal conductivity analyzer (Gow-Mac 10.747-I). The detector was previously calibrated using binary gaseous mixtures of known composition. The sensitivity of the analyzer depends on the difference of thermal conductivity between the two components and in the case of xenon + SF_6, is on the order of 0.0009 mole fraction. However, errors associated with sampling and calibrations bring the reproducibility of the results for different samples to ±0.003 mole fraction.

Temperature was measured using a platinum 100-Ω resistance thermometer previously calibrated (on ITS-90) against a standard 25-Ω platinum resistance thermometer. The final temperature reading accuracy lies within ±0.01 K above 230 K, ±0.02 K in the range of 224−230 K, and ±0.05 K below 224 K. The vapor pressures were measured using a Setra 205-2 transducer connected to a Prema 6001 multimeter, previously calibrated against a Ruska dead weight gauge (model 2417). The final pressure reading accuracy lies within ±1.3 kPa in the entire pressure range (up to 7 MPa).

The xenon gas used in this work was purchased from Air Liquide, and the SF_6, from Matheson. Both were used as received and have stated mass fraction purities of 0.999 95 and

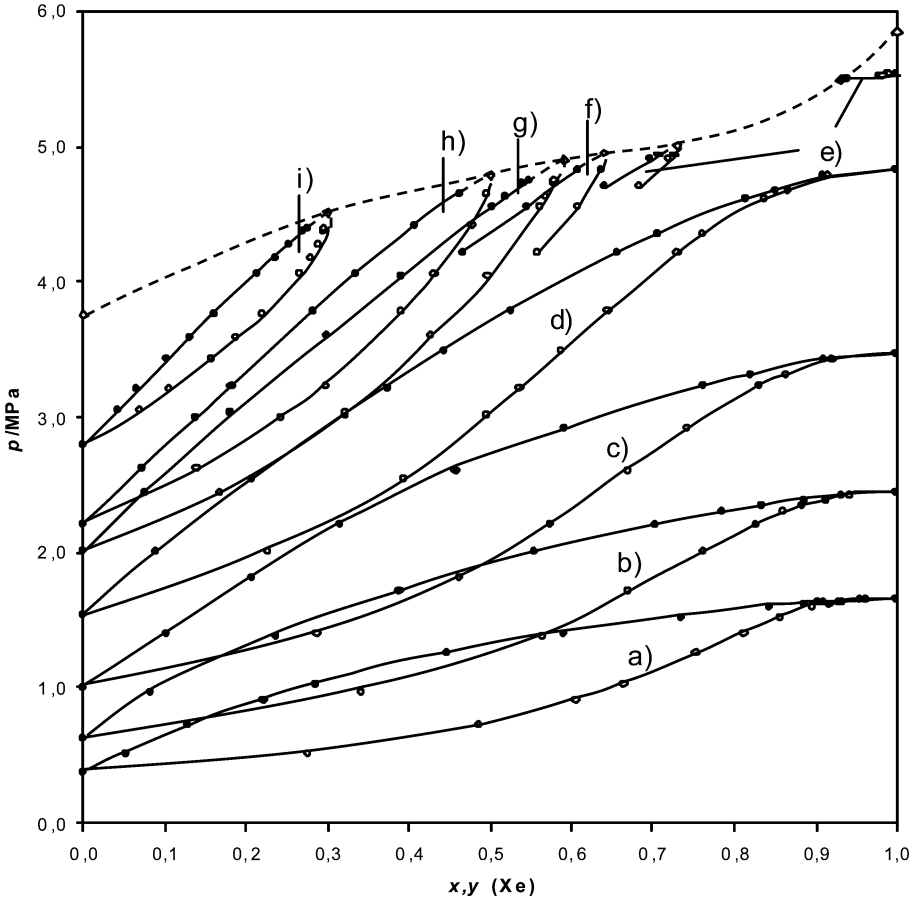

Figure 1. Constant-temperature $P(x, y)$ slices of the $x\mathrm{Xe} + (1 - x)\mathrm{SF_6}$ phase diagram. Solid lines are interpolations of the experimental results; the symbols correspond to the experimental data given in Tables 1 and 2: (a) 235.34, (b) 250.32, (c) 265.35, (d) 280.85, (e) 287.29, (f) 289.26, (g) 291.31, (h) 295.75, and (i) 305.27 K.

TABLE 3: Constants for the Redlich−Kister Equation (eq 1) and G^E for the Equimolar Mixtures Calculated Using Barker's Method

T (K)	A	B	C	G^E_x=0.5/J mol^{-1}
235.34	0.8978 ± 0.0037	−0.1220 ± 0.0077	0.036 ± 0.012	439.2 ± 1.6
250.32	0.7626 ± 0.0066	0.020 ± 0.014	0.078 ± 0.021	396.8 ± 1.1
265.35	0.5849 ± 0.0034	−0.0653 ± 0.0084	−0.091 ± 0.014	322.6 ± 1.0

0.9999, respectively. The vapor pressure of pure SF_6 was measured at several temperatures between 225 and 305 K. Our results are, on average, lower than those of Funke et al.[15] by up to 1.5%. It should be noted, however, that vapor pressure data for SF_6 from different authors can differ by as much as 4% within the same temperature range. The vapor pressure of pure xenon was measured between 189 and 283 K. The overall agreement with the values of Theeuwes and Bearman[16] is within 0.3% and 0.6% in the low-temperature limit. This difference can be explained by temperature differences ($T - T_{\mathrm{literature}}$) smaller than ±0.04 K, which lie within our bath temperature control in this range.

3. Results

The equilibrium vapor pressure and composition results (p, T, x, y) of the xenon + SF_6 binary mixtures at each temperature are recorded in Table 1 for the isotherms at temperatures lower than the critical temperature of xenon and in Table 2 for the isotherms between the critical temperatures of the two pure components. The complete set of isotherms is plotted in Figure 1. Table 1 also gives values of the difference between the experimental compositions of the gaseous phase and those calculated using Barker's thermodynamic consistency method,[17] in the form used by Calado et al.[18] For this purpose, second and third virial coefficients for xenon were taken from Streett et al.[19] Second virial coefficients for SF_6 were taken from the compilation of Dymond and Smith[20] and third virial coefficients were calculated from the correlation of Orbey and Vera.[21] The volumetric properties for liquid xenon were taken from Theeuwes and Bearman,[16] and those for SF_6, from Daubert and Danner.[22]

According to Barker's method, the parameters in the expression relating the excess Gibbs energy to composition, usually a Redlich−Kister expansion,

$$G^E/RT = x_1x_2[A + B(x_1 - x_2) + C(x_1 - x_2)^2]$$

are fitted by a least-squares procedure that minimizes the pressure residuals (the differences between the experimental and calculated pressures, which are also included in Table 1), using only p-x data. The parameters in the Redlich−Kister equation are then used to evaluate p-y data via the Gibbs−Duhem equation, and the results are compared with the experimental measurements. This procedure was restricted to the lowest pressure isotherms due to lack of reliable virial coefficients both for the pure components and mixtures. For this reason, the isotherm at 280.85 K was not included in this procedure. The obtained Redlich−Kister coefficients, as well as the values of G^E for the equimolar mixtures, are recorded in Table 3, and

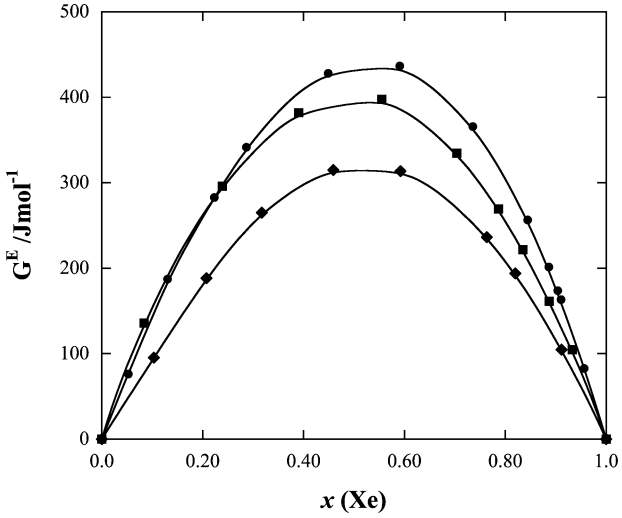

Figure 2. Excess molar Gibbs energies G^E for xXe + $(1 - x)$$SF_6$ at (●) 235.34, (■) 250.32, and (♦) 265.35 K.

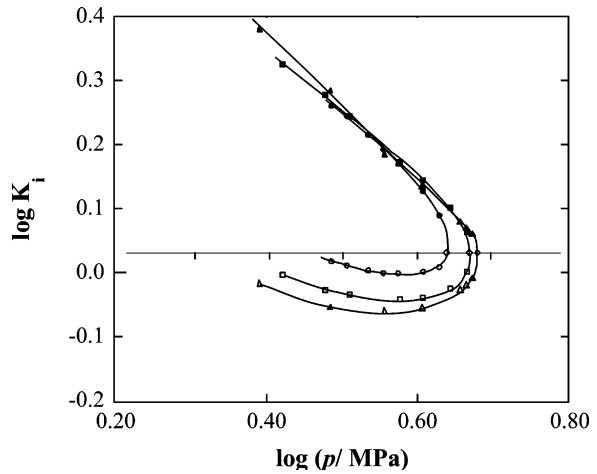

Figure 3. K diagram at three temperatures of the xXe + $(1 - x)$$SF_6$ phase equilibria: (△) 291.31, (□) 295.79, and (○) 305.27 K.

the G^E curves are plotted in Figure 2. From the temperature dependence of G^E, an average value of the excess molar enthalpy, H^E, can be estimated using the Gibbs−Helmholtz equation. For the equimolar composition, a value of $H^E = 1349 \pm 264$ J mol^{-1} was found.

The internal consistency of the data can also be observed in Figure 3 with the aid of the K-value plots, since these tend to exaggerate scatter in the results ($K_i = y_i/x_i$, where y_i is the mole fraction of component i in the vapor phase and x_i is the corresponding mole fraction in the liquid phase). These plots were also used for a better definition of the mixture critical line, since above the critical temperature of SF_6, the two branches converge and exhibit a vertical tangent at the mixture critical point where $K = 1$. The xenon + SF_6 critical line extrapolated by this method is shown as the dashed line in Figure 1. As can be seen, the line is continuous between the critical points of the pure components; hence, the system can be included in the type I classification of van Konynenburg and Scott.[13] The critical line exhibits a minimum in temperature (which can be better observed in a $p-T$ projection, as shown in Figure 5), which results in the isotherm at 287.29 K having two critical points. Since the isotherm at 280.85 K is continuous, the minimum must therefore lie between 280.85 and 287.29 K.

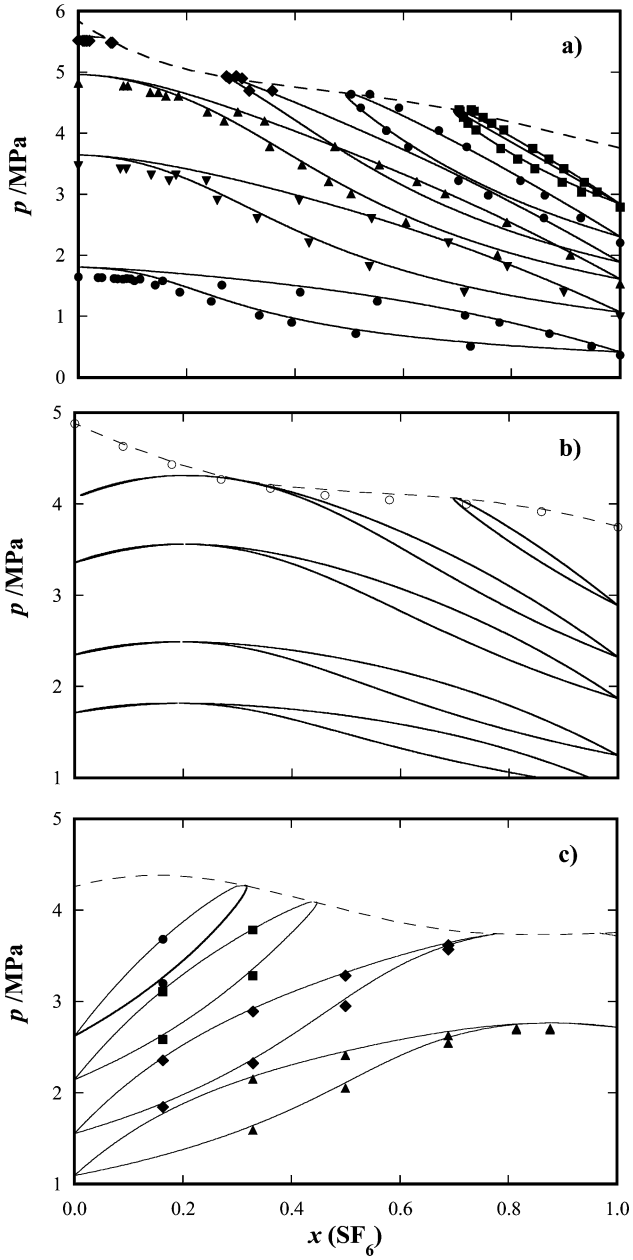

Figure 4. Constant-temperature $P(x, y)$ slices for (a) SF_6 + xenon, (b) SF_6 + ethane (from bottom to top, at 258.17, 270.92, 286.86, 296.1, and 305.98 K), and (c) SF_6 + propane (from bottom to top, at 303.15, 318.15, 333.15, and 343.15 K). Lines correspond to predictions obtained from the SAFT-VR equation of state. The symbols correspond to the experimental data given in Tables 1 and 2 in the case of SF_6 + xenon, in ref 28 in the case of the SF_6 + ethane mixture, and in ref 26 in the case of SF_6 + propane.

4. Discussion

A quantitative interpretation of the results was performed using the statistical associating fluid theory for potentials of variable range, SAFT-VR.[23,24] The SAFT-VR approach describes molecules as chains of m tangentially bonded hard spherical segments with the dispersion interactions modeled by a potential of variable attractive range, such as the square-well potential used in this work. Each segment is characterized by three parameters; namely the hard-sphere diameter, σ, and the depth, ϵ, and width, λ, of the potential well. A single sphere is naturally used to model the xenon atom.[7] The remaining pure substance parameters, σ, ϵ, and λ, are determined by fitting the theoretical expressions to experimental vapor pressure and

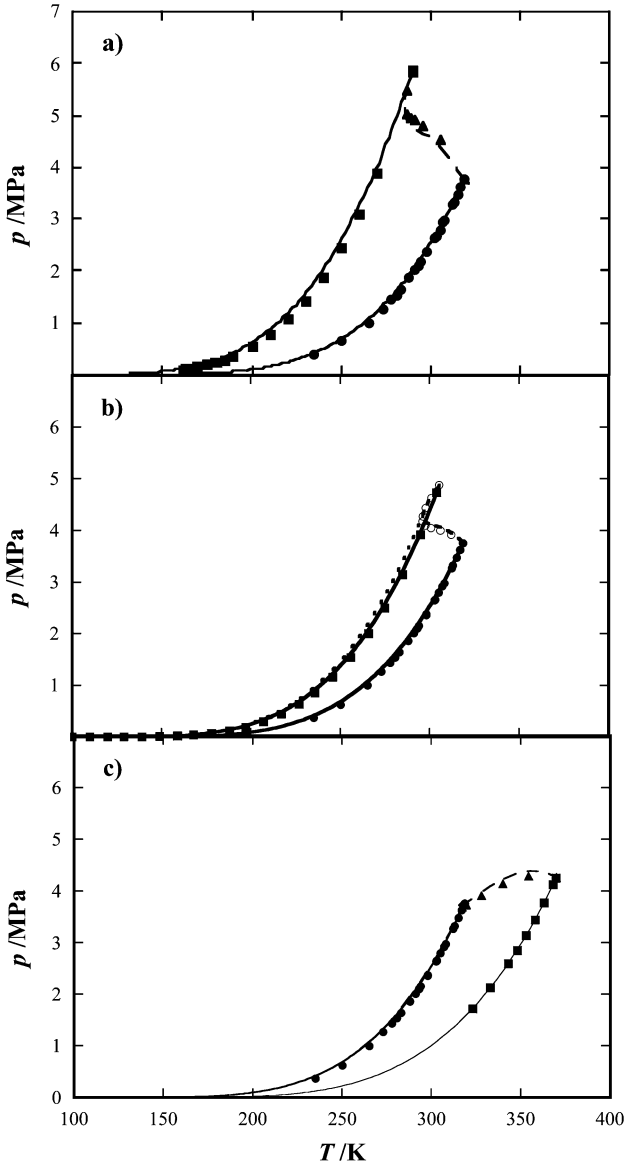

Figure 5. $p-T$ projection for (a) SF_6 (circle) + xenon (square), (b) SF_6 (circle) + ethane (square), and (c) SF_6 (circle) + propane (square) phase diagrams. The lines represent the SAFT-VR predictions.

TABLE 4: Optimized Square-Well Intermolecular Potential Parameters for SF_6 and Xenon[a]

substance	m	σ (nm)	ϵ/k (K^{-1})	λ
Xe	1.00	0.4243	225.9	1.478
SF_6[b]	1.46	0.4685	261.0	1.381

[a] m is the number of spherical segments in the model, λ is the range parameter, σ is the diameter of each segment, and ϵ/k isthe well depth. [b] Ref 30.

saturated liquid density data from the triple point, to the critical point. For SF_6, m was determined alongside the size and energy parameters from the fit to the pure substance properties. Since the SAFT-VR equation, like all analytical engineering equations of state, overpredicts the experimental critical point and we are interested in the whole phase diagram, including the critical region, the optimized parameters have been rescaled to the experimental critical point. The parameters for xenon were determined in previous work and are listed in Table 4, together with those of SF_6. We note, however, that the rescaling results in larger deviations from experimental data at lower temperatures and pressures. This shortfall has been addressed in a *crossover* version of the SAFT-VR equation of state (SAFT-VRX) for pure fluids and mixtures,[25] which accurately captures the crossover from classical to nonclassical behavior seen in real fluids. For details of the SAFT expressions, the reader is referred to the original SAFT-VR papers.[23,24]

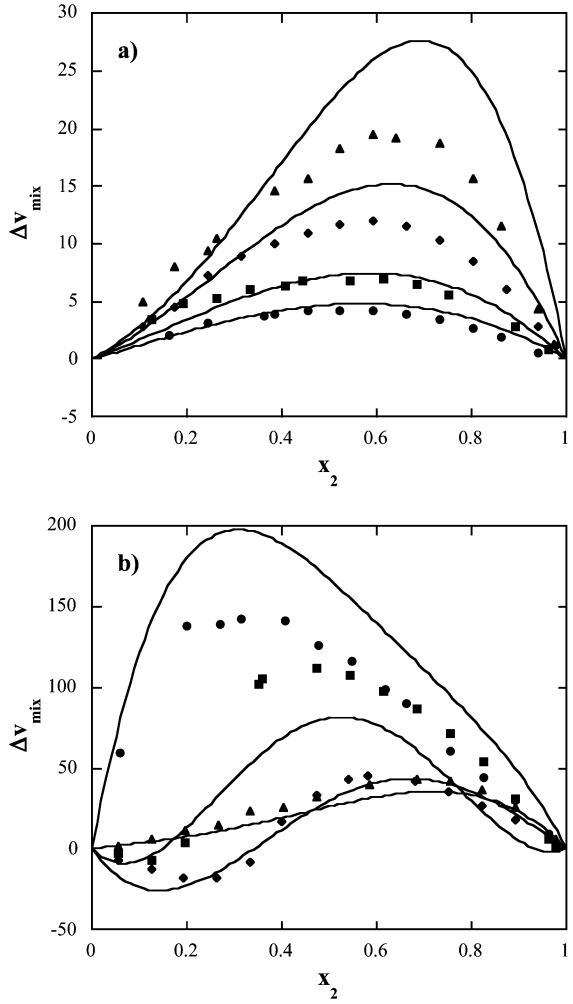

Figure 6. Excess volumes for the SF_6 + ethane binary mixture at (a) 4.88 MPa and $T = 250.15$, 270.15, 290.15, and 298.15 K (from bottom to top) and (b) 312.15 K and $p = 3.76$, 4.32, 4.88, 6.0 MPa (from top to bottom). Solid lines correspond to the SAFT-VR prediction, and the symbols, the experimental data of Wormald and co-workers.[27,28]

Constant temperature $p(x, y)$ slices of the xenon + SF_6 phase diagrams are presented in Figure 4a. A value of $\xi = 0.9139$, which was determined from a best fit to the experimental data, was used in the calculations. As can be seen from the Figure, the results are in excellent agreement with the experimental data. The phase compositions are well-described, as is the temperature dependence and the mixture critical line. In Figure 5a, we present the $p-T$ projection of the xenon + SF_6 fluid phase diagram as predicted by the SAFT-VR approach compared to the experimental data. As expected, and in agreement with the experimental observations, the theory predicts that the xenon + SF_6 binary mixture is a type I system. The minimum in the critical line is observed at 285 K, which agrees well with the experimentally observed interval of 280−287 K.

In relation to the current work, another class of interesting mixtures is generated by the substitution of xenon by a hydrocarbon. This follows from a recent finding that liquid xenon displays a behavior that resembles that of the *n*-alkanes when mixed with a number of substances, including perfluorinated compounds. These findings have been corroborated by the theory in a number of recent papers on the phase behavior

of binary systems involving xenon.[9,10,12] As previously mentioned, the calculated SAFT-VR parameters for xenon lie within the average value of those used to describe the *n*-alkanes; moreover, interaction parameters obtained for binary mixtures containing xenon can be transferred to the corresponding mixtures involving alkanes. If the analogy holds, the value of $\xi = 0.9139$ taken from the SF_6 + xenon system should apply to the corresponding SF_6 + *n*-alkane systems. Constant temperature *P-x,y* slices of the SF_6 + propane phase diagram are presented in Figure 4c and compared with experimental data.[26] As can be seen from the figure, using the cross interaction parameter determined for the xenon + SF_6 system, we are able to accurately predict the *P-x,y* isotherms, including the azeotropes. The $p-T$ projection of the phase diagram is shown in Figure 5c, and again, good agreement is achieved between the theoretical predictions and experimental data.

To further test this behavior, we examined the thermodynamic behavior of binary mixtures of SF_6 and ethane, which have recently been studied experimentally by Wormald and Hodgetts[27,28] and Horstmann et al.[29] Using the value of ξ obtained for the xenon + SF_6 system, we have predicted the excess volumes of binary mixtures of SF_6 and ethane (Figure 6) at near-critical and supercritical conditions. As can be seen from the Figure, the predictions are in good agreement with the experimental data at lower temperatures and reproduce the S-shaped V^E curves at higher pressures, but deviate at higher temperatures and lower pressures. Given that excess properties are among the most difficult physical properties to predict, the overall agreement can be considered quite good. Furthermore, it should be kept in mind that these are true predictions calculated with a ξ transferred from the xenon + SF_6 binary mixture and not fitted to the experimental data being studied. In Figures 4b and 5b, we present predictions for the phase diagram of the ethane + SF_6 binary mixture. Again, the agreement between the theory and experiment is excellent. It should be noted that the SF_6 + ethane system is, in a way, an intermediate case between SF_6 + xenon and SF_6 + propane, as shown by the evolution of the mixture critical lines and the appearance of the azeotrope in sequence.

Acknowledgment. L.M.B.D. thanks Fundação para a Ciência e a Tecnologia for financial support.

References and Notes

(1) Fonseca, I. M. A.; Lobo, L. Q. *Fluid Phase Equilib.* **1989**, *47*, 249.

(2) Machado, J. R. S.; Lobo, L. Q.; Gubbins, K. E.; Staveley, L. A. K. *J. Chem. Soc. Faraday I* **1980**, *76*, 2496.

(3) Lobo, L. Q.; McClure, D. W.; Staveley, L. A. K.; Clancy, P.; Gubbins, K. E.; Gray, C. G. *J. Chem. Soc. Faraday Trans. 2* **1981**, *77*, 425.

(4) Beret, S.; Prausnitz, J. M. *AIChE J.* **1975**, *21*, 1123.

(5) Chapman, W. G.; Gubbins, K. E.; Jackson, G.; Radosz, M. *Fluid Phase Equilib.* **1989**, *52*, 31.

(6) Chapman, W. G.; Gubbins, K. E.; Jackson, G.; Radosz, M. *Ind. Eng. Chem. Res.* **1990**, *29*, 1709.

(7) Filipe, E. J. M.; Gomes de Azevedo, E. J. S.; Martins, L. F. G.; Soares, V. A. M.; Calado, J. C. G.; McCabe, C.; Jackson, G. *J. Phys. Chem. B* **2000**, *104*, 1315.

(8) Filipe, E. J. M.; Martins, L. F. G.; Calado, J. C. G.; McCabe, C.; Jackson, G. *J. Phys. Chem. B* **2000**, *104*, 1322.

(9) Dias, L. M. B.; Filipe, E. J. M.; McCabe, C.; Calado, J. C. G. *J. Phys. Chem. B* **2004**, *108*, 7377.

(10) McCabe, C.; Dias, L. M. B.; Jackson, G.; Filipe, E. J. M. *Phys. Chem. Chem. Phys.* **2001**, *3*, 2852.

(11) Bonifácio, R. P.; Filipe, E. J. M.; McCabe, C.; Gomes, M. F. C.; Pádua, A. A. H. *Mol. Phys.* **2002**, *100*, 2547.

(12) Filipe, E. J. M.; Dias, L. M. B.; Calado, J. C. G.; McCabe, C.; Jackson, G. *Phys. Chem. Chem. Phys.* **2002**, *4*, 1618.

(13) van Konynenburg, P. H.; Scott, R. L. *Philos. Trans. R. Soc. London A* **1980**, *298*, 495.

(14) Streett, W. B.; Calado, J. C. G. *J. Chem. Thermodyn.* **1978**, *73*, 527.

(15) Funke, M.; Kleinrahm, R.; Wagner, W. *J. Chem. Thermodyn.* **2002**, *34*, 735.

(16) Theeuwes, F.; Bearman, R. J. *J. Chem. Thermodyn.* **1970**, *2*, 507.

(17) Barker, J. A. *Aust. J. Chem.* **1953**, *6*, 207.

(18) Calado, J. C. G.; Chang, E.; Streett, W. B. *Physica A* **1983**, *117*, 127.

(19) Streett, W. B.; Sagan, L. S.; Staveley, L. A. K. *J. Chem. Thermodyn.* **1973**, *5*, 633.

(20) Dymond, J. B.; Smith, E. B. *The Virial Coefficients of Pure Gases and Mixtures*; Clarendon Press: Oxford, 1980.

(21) Orbey, H.; Vera, J. H. *AIChE J.* **1983**, *29*, 107.

(22) Daubert, T. E.; Danner, R. P. *Physical and Thermodynamic Properties of Pure Chemical Data Compilations*; Taylor and Francis: Philadelphia, PA.

(23) Gil-Villegas, A.; Galindo, A.; Whitehead, P. J.; Mills, S. J.; Jackson, G.; Burgess, A. N. *J. Chem. Phys.* **1997**, *106*, 4168.

(24) Galindo, A.; Davies, L. A.; Gil-Villegas, A.; Jackson, G. *Mol. Phys.* **1998**, *93*, 241.

(25) McCabe, C.; Kiselev, S. B. *Fluid Phase Equilib.* **2004**, *3*, 219. McCabe, C.; Kiselev, S. B. *Ind. Eng. Chem. Res.* **2004**, *43*, 2839. Sun, L. X.; Zhao, H. G.; Kiselev, S. B.; McCabe, C. *Fluid Phase Equilib.* **2005**, *275*, 228. Sun, L. X.; Zhao, H. G.; Kiselev, S. B.; McCabe, C. *J. Phys. Chem. B* **2005**, *109*, 9047.

(26) Clegg, H. P.; Rowlinson, J. S. *Trans. Faraday Soc.* **1955**, *51*, 1327.

(27) Wormald, C. J.; Hodgetts, R. W. *Fluid Phase Equilib.* **2001**, *192*, 121.

(28) Wormald, C. J.; Hodgetts, R. W. *J. Chem. Thermodyn.* **2002**, *34*, 875.

(29) Horstmann, S.; Fischer, K.; Gmehling, J. *AIChE J.* **2002**, *48*, 2350.

(30) We note that the size parameter reported in ref 10 for SF_6 was the optimized rather than the rescaled value, with a corresponding energy parameter of 278.7 K.